

# Quasimetallic behavior of carrier-polarized C<sub>60</sub> molecular layers: Experiment and theory

Z. H. Lu, C. C. Lo, C. J. Huang, and Y. Y. Yuan

*Department of Materials Science and Engineering, University of Toronto, 184 College Street, Toronto, Ontario Canada, M5S 3E4*

M. W. C. Dharma-wardana\* and Marek Z. Zgierski

*National Research Council of Canada, Ottawa Canada, K1A 0R6*

(Received 28 June 2005; revised manuscript received 16 September 2005; published 28 October 2005)

Although C<sub>60</sub> is an insulator with a band gap  $E_g$  of  $\sim 2.5$  eV, we show experimentally and theoretically that  $E_g$  is strongly affected by image forces and injected charges. In sharp contrast to the Coulomb blockade typical of quantum dots,  $E_g$  is *reduced* by Coulomb effects. The conductance of a micron-sized C<sub>60</sub> film sandwiched between metal (Al, Ag, Au, Mg, and Pt) contacts is investigated. Excellent Ohmic conductance holds for C<sub>60</sub> layers at room temperature, on using Al/LiF bilayer contacts. Arrhenius type activated conductivity with an activation gap of  $\sim 0.16$  eV is found.

DOI: 10.1103/PhysRevB.72.155440

PACS number(s): 73.61.Wp, 05.30.Fk, 71.10.Pm, 71.45.Gm

## I. INTRODUCTION

The Fullerene C<sub>60</sub> solid is a molecular crystal<sup>1</sup> with a band gap of  $\sim 2.5$  eV. The energy gap between the highest occupied molecular orbital (HOMO) and the lowest unoccupied molecular orbital (LUMO) of the *isolated* C<sub>60</sub> molecule is even larger. Alkali-metal doping of the solid makes it a conductor or a superconductor.<sup>2</sup> Other methods of converting C<sub>60</sub> into a conductor involve exotic chemical routes where, e.g., C<sub>60</sub> molecules are joined by metal-ligand structures.<sup>3</sup> Such efforts focus on improving the conductance of the molecular layer itself. Another important factor is the electrical contact between the molecular layer and the metal surface. Such contacts, unless properly formed, may induce chemical processes that lead to fragmentation of the molecules themselves.<sup>4,5</sup>

Unlike quantum dots and related nanostructures where a major problem is to make sufficiently “identical” or equivalent copies, molecules are already equivalent copies. Unlike quantum dots whose energy levels are in the millivolt range, molecules have energy levels which are robust at room temperature. Fullerenes have been examined as a class of model molecules which may have great potential for molecular electronics.<sup>6,7</sup> Many studies on theoretical C<sub>60</sub> devices have emphasized the control of conductance using scanning-tunneling probes, electromechanical, and other gates.<sup>8</sup> In the simulation by Taylor *et al.*,<sup>8</sup> a single C<sub>60</sub> molecule is positioned between two Al leads. In this ideal device, metallic conductance occurs when the triad of degenerate LUMO acquires three electrons forming a half-filled band; the LUMO is  $\sim 1.8$  eV above the HOMO in their local-density approximation (LDA).

Given that *single-molecule* current ( $I$ ) and voltage ( $V$ ) data are perhaps controversial,<sup>4</sup> we turn to  $I$ - $V$  data for pure micron-sized C<sub>60</sub> films. Usually the top contact is formed by depositing hot-metal vapor onto the C<sub>60</sub> film preformed on a cold metal surface. Metal vapors contain metal atoms which are far more reactive than the metal in the solid state where the metal is in the form of ions which are immersed in a sea of electrons. Hence we emphasize the need to protect the C<sub>60</sub>

film from hot metal atoms during device fabrication. Studies of C<sub>60</sub> on crystallographically controlled surfaces of Al, Ag, Au, Mg, etc.,<sup>9–11</sup> have been carried out by depositing the C<sub>60</sub> on the *cold* substrate and hence the above problem does not arise in such studies. Scanning-tunneling microscopy (STM) and photoemission studies of C<sub>60</sub> layers deposited on *hot* Al surfaces<sup>12</sup> show clear surface reconstruction and interaction of the Al surface with the first C<sub>60</sub> monolayer. Hence we make a special effort to protect the surfaces and ensure that the C<sub>60</sub> molecules do not encounter hot metal atoms. However, even with hot surfaces, studies show that charge transfer and bonding modifications occur within the first C<sub>60</sub> monolayer, i.e., the layer in contact with the metal, while the second monolayer usually remains unaffected,<sup>13,14</sup> except for weaker physical effects. In effect C<sub>60</sub> is highly polarizable and screens out long-ranged fields. We call this physico-chemically modified interface-layer the *metal-fulleride* layer. Metal-fulleride formation for C<sub>60</sub> on Al, as well as for Al deposition on C<sub>60</sub> has been studied by, e.g., Owens *et al.*<sup>9</sup> Pt and Ni surfaces are more complex; they form strong bonds with C<sub>60</sub> and catalyze the decomposition of the organic molecule at sufficiently high temperatures.<sup>15</sup>

Reports<sup>16</sup> of  $I$ - $V$  data on such *metal/C<sub>60</sub>/metal* sandwich structures suggest semiconducting, rectifying, or insulating behavior. Previously<sup>17</sup> we showed how an ultrathin layer of LiF dramatically modifies the  $I$ - $V$  characteristics of a molecular film by (i) protecting the organic molecules from reactions with the metal, (ii) creating a sharp electrode density of states (DOS) favoring carrier injection into unoccupied states of the molecule. Similar effects of ionic epilayers on metals are not uncommon.<sup>18</sup> Here we show that polarization and charge-injection effects dramatically change the “insulating” or semiconducting character of C<sub>60</sub> films. We find that low-work function metals like Al, Ag, and Mg sandwiching C<sub>60</sub> layers and protected with LiF interface layers show quasimetallic  $I$ - $V$  characteristics, i.e.,  $I$  varying essentially linearly with the applied bias  $V$ , for both forward and reverse bias. However, the temperature dependence of the current for a given bias reveals that the conductance is not truly metallic, but controlled by a small activation energy of  $\sim 0.16$  V.

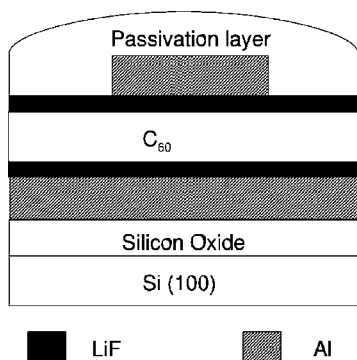


FIG. 1. A schematic of the device showing LiF protected Al electrodes sandwiching a  $C_{60}$  layer. Note that the Al strips are orthogonally positioned.

The plan of the paper is as follows. We present the experimental details and results in Sec. II. As we are dealing with  $C_{60}$ , a very large molecule (760 electrons), we can only present a theoretical analysis which cannot encompass the actual geometry of the device. However, a theory which clarifies the salient features of the observations is presented in Sec. III, using detailed electronic structure calculations for the  $C_{60}$  molecule as well as image-charge interaction models and results of photoelectron and STM experiments available in the literature. These show that the insulating energy gap of the isolated molecule is strongly reduced by the presence of the metallic electrode and the charge injected onto an adjacent  $C_{60}$  by the applied bias. In effect, the reduction of the HOMO-LUMO gap, together with the alignment of the LUMO level with the Fermi energy of low-work function metals is sufficient to understand the observed quasimetallic behavior of these  $C_{60}$  films. This section is followed by a concluding discussion, summarizing our experimental and theoretical results.

## II. EXPERIMENTAL DETAILS AND RESULTS

Details of sample fabrication etc., are given in Lu *et al.*<sup>17</sup> A schematic diagram of the morphology of the device is shown in Fig. 1. The devices were made on  $2 \times 2$  in Si(100) wafers with 2000 nm furnace oxides on top. The first metal (Al, Mg, Ag, Au, Pt) electrode (“bottom electrode”), is 1 mm wide, 50 mm long, and 60 nm thick. It was deposited through a shadow mask, and the  $C_{60}$  films were then deposited over the bottom electrode. A second metal (Al) electrode, 1 mm wide, 50 mm long, and 100 nm thick, (the “top electrode”), was deposited over the  $C_{60}$  films. An ultrathin layer ( $\sim 1$  nm) of LiF was deposited on the  $C_{60}$  film prior to the deposition of the top electrode. The top metal lines were orthogonal to the bottom metal lines so that each intersection of two lines produces one *metal/C<sub>60</sub>/metal* device. There are 20 to 100 devices on each wafer. A final silicon oxide film of  $\sim 300$  nm encapsulated the device. This final encapsulation is essential to produce consistent and reproducible results, since contamination with air has a drastic effect.<sup>19</sup> All devices were made in a cluster tool using high-vacuum techniques.<sup>17</sup> The figure shows LiF layers interfacing the bot-

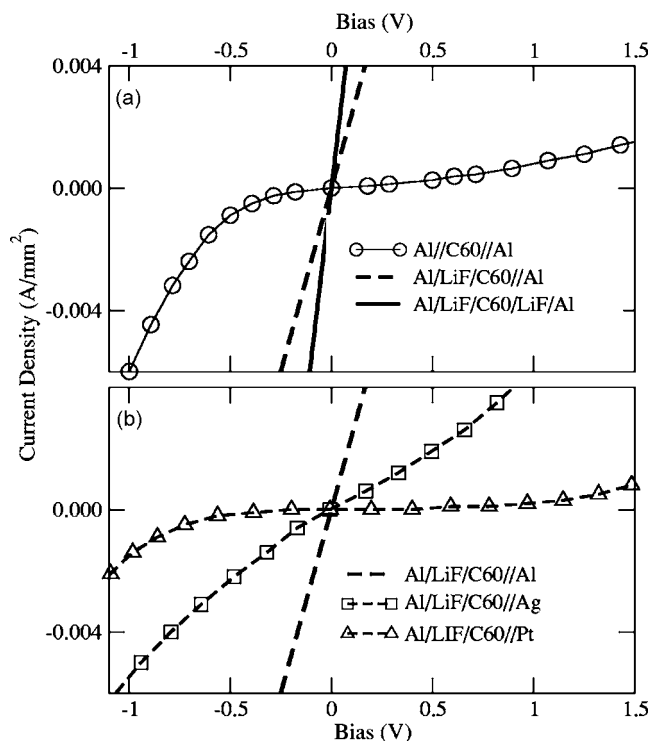


FIG. 2. (a)  $I$ - $V$  curves for three Al/ $X$ / $C_{60}$ (250 nm)/ $X$ /Al devices, with  $X$ =LiF or left unprotected ( $//$ ) at the top and bottom interlayers. (b)  $I$ - $V$  curves for Al/LiF/ $C_{60}$ (250 nm)// $M$ , with  $M$  = Al, Ag, and Pt. Only the top electrode has LiF.

tom electrode as well as the top electrode. However, we fabricated devices where the LiF layer at the bottom electrode and/or the top electrode were omitted and the  $I$ - $V$  curves were determined to examine the role of the LiF layers.

The  $I$ - $V$  measurements were in a dark ambient, using an HP4140B meter with a Materials Development probe station. The measured  $I$ - $V$  curves as a function of the temperatures<sup>19</sup> were quite reproducible from one thermal cycle to another and very nearly symmetrical for reverse bias when protective LiF interface layers were used.

Figure 2(a) shows  $I$ - $V$  data for samples with or without LiF interlayers. In samples with bare-Al, i.e., Al// $C_{60}$ //Al the left-hand Al (the “top”) electrode was formed by Al vapor on  $C_{60}$ , while the right-hand Al (“bottom”) electrode was cold during  $C_{60}$  deposition. In such systems the fulleride interlayers formed by interaction with hot metal atoms are uncontrolled, and interfaces without LiF are denoted by  $//$ , a double bar. In devices with LiF at the top, i.e., Al/LiF/ $C_{60}$ //Al, the  $C_{60}$  is protected from hot-metal deposition. The bare-Al devices produce a typical diodelike  $I$ - $V$  behavior (see Fig. 2, top panel) with negligible current flow at low bias, and asymmetric under reverse bias. The use of a LiF interlayer at the top (“hot”) electrode is enough to create a quasimetallic (linear  $I$ - $V$ ) device with *zero threshold* for current flow. When LiF is interfaced at the bottom electrode as well, the conductance ( $I/V$ ) improves only slightly, showing that the bottom electrode, where  $C_{60}$  was deposited in the cold, needs no protection. The behavior is Ohmic, with no discontinuity in the constant gradient  $I/V$  on reversing the bias. This was confirmed for  $C_{60}$  films varying from

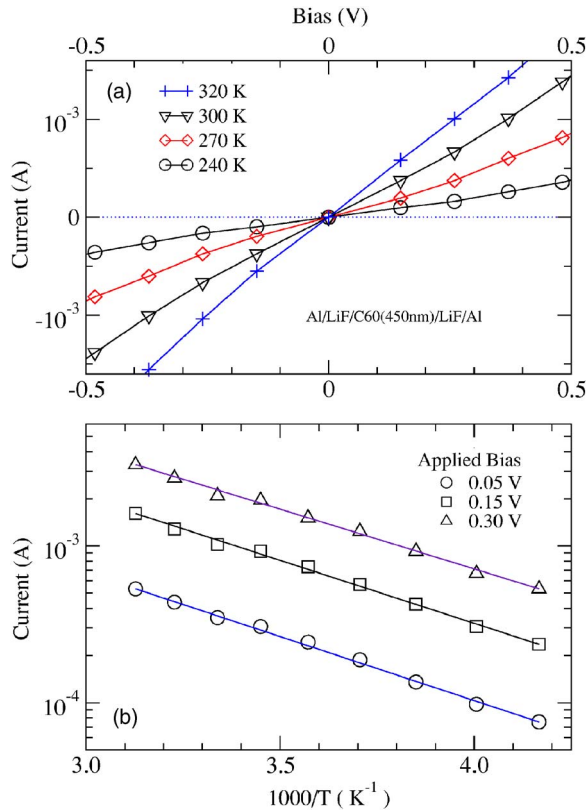


FIG. 3. (Color online) (a)  $I$ - $V$  curves showing increased nonlinearity at lower  $T$ , for an Al/LiF/C<sub>60</sub>(450 nm)/LiF/Al device. (b) Arrhenius plots of the current as a function of  $1/T$ , over a range of  $\sim 100^\circ$ . The activation energy is  $0.155 \pm 0.005$  eV.

100 to 450 nm in thickness. Al<sup>3+</sup> migration cannot be the cause of the conductance since such migration is obstructed by the LiF layer. Figure 2(b) shows typical results for Al, Ag, and Pt, with Al and Ag quasimetallic. Metal-like  $I$ - $V$  is achieved for  $M$ =Al, Ag, and Mg at room temperature. Thus  $I$  depends linearly on  $V$ , for both forward and reverse bias. When  $M$ =Pt, the conductance is very small, nonlinear and strongly asymmetric for reverse bias. The work functions for polycrystalline Mg, Ag, Al, Au, and Pt are 3.7, 4.3, 4.3, 5.1, and 5.7 eV, respectively.<sup>20</sup> While Ag and Al have essentially the same work function, the electron density in Al is  $\sim 3$  times higher. These results show that quasi-Ohmic  $I$ - $V$  is found for low-work-function (LWF) metals, while other considerations apply for gold<sup>21</sup> and Pt.

A true metallic conductor not only shows linear  $I$ - $V$  (i.e.,  $R=V/I$  remains constant) behavior, but also shows a decreasing resistance with decreasing temperature. The temperature dependence of the current  $I$  in these C<sub>60</sub> films for a given bias reveals that the conductance is in fact not truly metallic, but involves a small activation energy. In effect the C<sub>60</sub> film appears metallic at room temperature and semiconducting at low  $T$  (see Fig. 3). The  $T$  dependent  $I$ - $V$  data show an  $I=A \exp(-\Delta E/k_b T)$  Arrhenius behavior with an activation energy of  $\sim 0.16$  eV, consistent with the theory discussed below.

### III. THEORY

A comprehensive theoretical treatment of the experimental structure would require (a) simulation of the Al/C<sub>60</sub> interface with and without a monolayer of LiF and (b) with at least several C<sub>60</sub> monolayers to represent the organic film. There is no translational invariance in the  $z$  direction (growth direction of the film), while there is nominal lattice periodicity in the  $x$ - $y$  directions parallel to the plane of the metal surfaces. However, as seen from the STM studies of Johansson *et al.*,<sup>12</sup> for C<sub>60</sub> deposited on hot-Al surfaces, the calculation of *even one monolayer* of C<sub>60</sub> needs to address the possibility of a  $2\sqrt{3} \times 2\sqrt{3}$  or  $6 \times 6$  surface reconstructions which require dealing with 36 Al atoms in each substrate layer, and possibly three or more C<sub>60</sub> molecules in the surface unit cell. The C<sub>60</sub> molecules may also take many configurations, e.g. positioning with a 6,6 bond, a 5,6 bond, or a pentagonal face on the surface etc., and show different orientations to each other. Such a calculation, which requires geometry optimization of at least two of the Al layers and the C<sub>60</sub> nuclear positions is totally beyond the capacity of any laboratory at present. Instead we exploit the following experimental observations to justify a simplified jellium-slab approach coupled with a detailed molecular-structure calculation for a “two-ball” model. They are

(i) C<sub>60</sub> layers deposited on cold bare Al surfaces with or without LiF show very similar quasi-Ohmic  $I$ - $V$ .

(ii) C<sub>60</sub> layers deposited on cold bare Ag surfaces are very similar to those of the aluminum system if suitably scaled.

(iii) Ag and Al polycrystalline surfaces have nearly identical work functions.

(iv) Hence photoelectron and STM results, and theoretical work on Ag/C<sub>60</sub> layers may be a useful guide to the behavior of Al and similar low work-function metals which are protected from direct interaction with C<sub>60</sub> via a monolayer of LiF.

(v) Even in hot deposited Al/C<sub>60</sub> where there is strong surface reconstruction, the inter-C<sub>60</sub> distance in the  $x$ - $y$  plane remains  $\sim 10$  Å, as in the pure C<sub>60</sub> solid, while the  $z$  direction is somewhat modified. This clearly shows that the lateral interactions are *not* important to the energetics of the C<sub>60</sub> layer, while the  $z$  direction is important. This experimental fact is also confirmed by DFT calculations for the Ag/C<sub>60</sub> system,<sup>11</sup> where a single C<sub>60</sub> molecule on a Ag surface has been treated.

(vi) Photoelectron studies of Ag, Al, and other low-work-function metals in contact with C<sub>60</sub> clearly show that the LUMO of the first monolayer is partially occupied by electrons transferred from the metal surface, splitting, and broadening the LUMO and HOMO levels.

Al is a high electron-density metal with the electron sphere radius  $r_s = [3/(4\pi\bar{n})]^{1/3} = 2.07$  in atomic units, where  $\bar{n}$  is the mean electron density. Hence the jellium model is usually an excellent model for an Al slab. Lang and Kohn have presented DFT calculations<sup>22</sup> and shown the applicability of the jellium model to simple metal surfaces. C<sub>60</sub> is also a high-electron density material, with 60 mobile electrons in a volume of radius  $\sim 3.5$  Å. This corresponds to an  $r_s \sim 1.7$ , i.e., a highly polarizable  $\pi$ -electron droplet held in place by the neutralizing carbon cage. Thus an image-charge model

would be an excellent approximation to the interaction between the Al slab and the  $C_{60}$  layer, as long as chemical interactions between the Al and the  $C_{60}$  are avoided. The image charges create a “built-in” electric field which lowers the Coulomb repulsion to charge transfer into the  $C_{60}$  molecule.<sup>23</sup> The Thomas-Fermi screening length  $\lambda = \sqrt{r_s}/0.815$  a.u., corresponding to the Al and  $C_{60}$  electron sphere radii of 2.07 and 1.7 are approximately 1 Å and 0.85 Å, respectively. This clearly shows that the image-charge fields set up by the interaction between the Al surface and the  $C_{60}$  are completely screened out by the first monolayer of  $C_{60}$  itself. A more conservative estimate of the screening length is obtained if the screening function of the  $C_{60}$  were calculated using a dipole polarizability model. Here again, the dipole polarizability  $\alpha$  of  $C_{60}$  is exceptionally large, being  $90 \text{ \AA}^3$  per molecule,<sup>24</sup> with a  $C_{60}$  diameter of about 7 Å. Thus screening occurs within one monolayer. This is also confirmed by photoemission data which show that only the first monolayer is affected.

This leaves us with the dilemma of explaining how the polarizing effect of the metal surface, screened out by the very first monolayer of  $C_{60}$  could have an effect on the subsequent electron transport in the film. That is, the simple but accurate image-charge picture shows that the  $C_{60}$  molecules dramatically lower their energy gap when near a LWF metal surface.<sup>23</sup> However, even if the first  $C_{60}$  monolayer (fulleride layer) adjusts to the Fermi energy of the metal and acquires electrons from the metal (as indicated by experiments<sup>14</sup> and by the image-charge picture) conduction in the film cannot occur without further charge transfer from  $C_{60}$  to  $C_{60}$ .<sup>25</sup> This requires us to examine what happens when a  $C_{60}$  layer already charged with electrons is adjacent to another  $C_{60}$  layer. Since there are no electric fields parallel to a metal surface or a highly polarizable layer, we need not consider the lateral interactions between a  $C_{60}$  and its neighbors in the  $x$ - $y$  plane. The applied bias as well as the electric field associated with the image charge acts in the  $z$  direction. Hence we simplify the full two-layer calculation and consider the model of two fullerene molecules as representing the uniaxial symmetry of the device, where the interball direction mimics the  $z$  axis. This is actually a very good approximation since the main effect of molecules around the axial pair is merely to contribute to the local field correction of the polarizability. This is also in conformity with the experimental observation that the ball-ball separation in the  $x$ - $y$  plane remains close to the 10 Å value found in bulk  $C_{60}$ .

In the following we show that the  $C_{60}$  layer polarized by the metal acts as a quasimetallic surface for polarizing the adjacent  $C_{60}$  layer. This inductive effect spreads into the film, lowering its  $E_g$ , while the applied bias  $V$  ensures the flow of charge. Thus while neutral  $C_{60}$  behaves as a *molecular crystal in photoemission* experiments,<sup>1</sup> our experiments and calculations show that room-temperature  $C_{60}$  behaves as a *quasimetal in the presence of polarizing carriers or metallic surfaces*.

In metals like Pt where metal  $d$  orbitals are involved, the physical situation is different and electron injection is negligible under low bias. Here strongly nonlinear  $I$ - $V$  is observed.

### Theoretical estimates of HOMO-LUMO gaps

We calculated the HOMO-LUMO gap  $E_g$  and the electronic density of states (DOS) for the  $C_{60}$  molecule, for  $C_{60}$ -LiF,  $C_{60}$ - $C_{60}$ ,  $C_{60}$ - $C_{60}^-$ , and  $C_{60}$ - $C_{60}^+$  structures, where the short bar  $-$  stands for all the interactions between the two moieties. The electronic structures are obtained from density functional calculations using the GAUSSIAN98 code<sup>26</sup> at the BP86/6-31G\* level.<sup>26,27</sup> Here BP86 refers to the exchange-correlation functional of Becke, Parr, and collaborators, while 6-31G\* refers to the Gaussian basis set selected for this study, available within the implementation of the GAUSSIAN98 code. The calculations included geometry optimization via total energy minimization using gradient corrected exchange-correlation functionals. Note that these procedures are quite superior to band structure-type calculations that may be applied to periodic  $C_{60}$  systems using plane-wave basis sets. The Becke-Parr type exchange-correlations functionals may of course be used for such calculations as well. However, the energy-gap estimates are less satisfactory because the self-interaction corrections, which are effective with localized basis sets, are not realized within the plane-wave scheme.

The DOS of some of the  $C_{60}$  structures are shown in Fig. 4, and  $E_g$  data are given in Table I. In Fig. 4(a) we compare our isolated-molecule DOS with the experimental results<sup>10</sup> for multilayers of  $C_{60}$  on Ag from direct and inverse photoemission (UPS and IPS). Thus the HOMO part of the experiment is from UPS (energy resolution  $\sim 0.1$  eV), and the LUMO part is from IPS (energy resolution  $\sim 0.3$  eV). We have positioned the DOS curves so that our calculated HOMO (H) and LUMO (L) peaks align with the experimental H and L peaks. The good agreement confirms the accuracy of our calculations.

LiF itself produces a decrease in the  $C_{60}$   $E_g$ , and may help to metallize the first  $C_{60}$  monolayer. The energy gaps  $E_g$  given in Table I are better than the band-structure LDA gaps. The BS-LDA gap for  $C_{60}$  is only  $\sim 1.8$  eV, and differs from the experimental solid-state gap of  $\sim 2.5$  eV. Our calculations show a spin-polarized level structure for the anion. This may have spintronics applications using suitable  $C_{60}$  systems,<sup>28</sup> since the spin gap of  $\sim 0.02$  eV is comparable to energies of quantum dots which have been proposed for spintronic applications.

Photoemission data<sup>9,10</sup> establish the metallization of the first  $C_{60}$  layer on metals such as Ag and Al, with as much as 1.8 electrons transferred<sup>29</sup> to the LUMO in the case of Ag. Hence the Hubbard on-site repulsion has been reduced from that of the isolated molecule. Thus to a first approximation, for low-work-function metals, the  $C_{60}$  molecular layer creates an image field which drives some electrons into the LUMO of the first  $C_{60}$  layer. This layer now acts as a quasimetallic layer to the second  $C_{60}$  layer, and induces image forces and metallizes the latter. This inductive process would become progressively weak, except for the applied bias which generates a net electron flow from layer to layer. The image-force model is only a first approximation. We present a full quantum calculation to demonstrate the reduction of the energy gap of a  $C_{60}$  molecule when it is positioned ( $\sim 10$  Å) close to another  $C_{60}$  molecule which carries a mo-

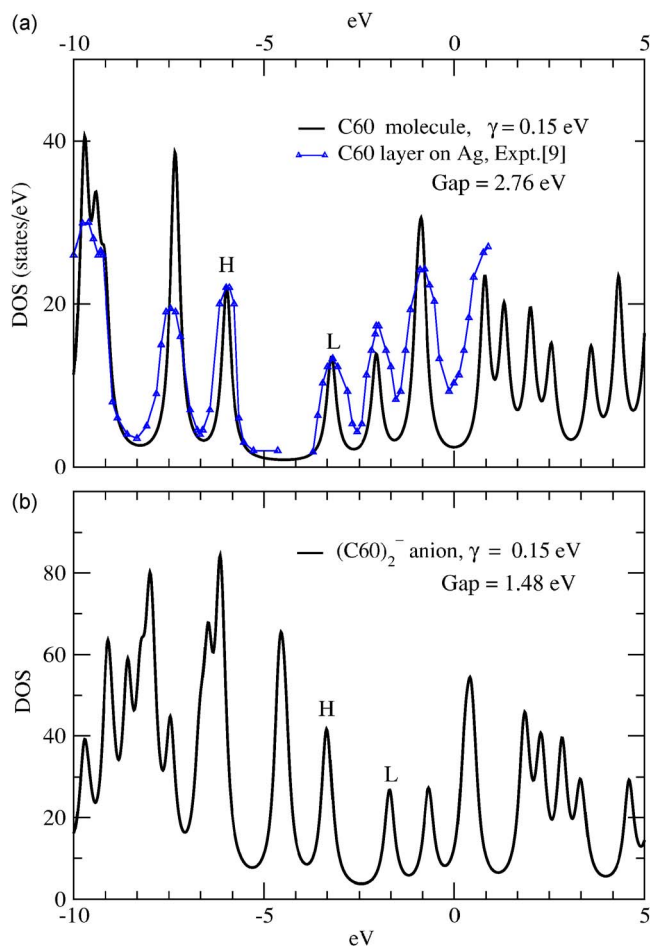


FIG. 4. (a) (Color online) The electron density of states (DOS) for isolated  $C_{60}$  near the energy gap. Experimental data (Ref. 10) for  $C_{60}$  on Ag are also shown. (b) DOS for the  $C_{60}^-C_{60}^-$  anion; the gap is further lowered by  $\sim 1.3$  V. A level width  $\gamma=0.15$  eV is assumed in the DOS calculations. See Table I.

bile charge in its LUMO. Each molecule is surrounded by molecules on all sides, and a multimolecular crystal Hamiltonian can be formulated if molecular pair interactions are known. We consider a pair of  $C_{60}$  molecules, mimicking two adjacent layers, with an electron injected to one of them. The

TABLE I. The HOMO, LUMO energies  $E_L$  and  $E_H$ , for the  $C_{60}$  system. The LiF axis is centered orthogonal to a  $C_{60}$  hexagon. The  $C_{60}-C_{60}$  intercenter distance is  $10.2 \text{ \AA}$ . The “LUMO” of the anion has an electron, and the “HOMO” of the cation has a hole. The  $E_g$  are from BP86/6-31G\* and not from LDA. The  $\alpha, \beta$  refer to spin states of the ion.

System	$E_H$ (a.u.)	$E_L$ (a.u.)	$E_g$ (eV)
$C_{60}$	-0.22003	-0.11854	2.8
$C_{60}-LiF$	-0.18993	-0.16157	0.8
$C_{60}^-C_{60}^- \alpha$	-0.11880	-0.06443	1.48
$C_{60}^-C_{60}^- \beta$	-0.11736	-0.06213	1.50
$C_{60}^+C_{60}^+ \alpha$	-0.28683	-0.23093	1.52
$C_{60}^+C_{60}^+ \beta$	-0.28485	-0.22942	1.51

final state of such a system is the  $(C_{60}^-C_{60}^-)$  anion, and shows a highly reduced gap. The reduction in  $E_g$  can be understood using the results of our calculation. The gap reduction arises from (a) splitting of the fivefold HOMO and the threefold LUMO multiplets by the electric field of the mobile charge in the metallized layer, (b) polarization and distortion of the molecules which persist under stationary state conditions, and (c) resulting modification of the on-site Coulomb interactions. Many of these issues have been examined using Hubbard-type models<sup>23</sup> of the film, or DFT calculations for a  $C_{60}$  molecule on Ag.<sup>11</sup> Hesper *et al.*<sup>23</sup> used an image-charge model for  $C_{60}$  on Ag to obtain a gap reduction of  $\sim 1.44$  eV. They even mention the possibility of “driving the insulator into the metallic state.” Hence, the present results have been anticipated by previous workers using simpler models. Our density-functional calculation for two  $C_{60}$  molecules involves nearly 500 electrons and is a very large calculation. It provides the parameters for constructing simpler, tight-binding or Hubbard models. The simpler models can be used to include the effect of other neighbors in the molecular film. However, we already presented our reasons for believing that lateral interactions, from the molecules on the  $x$ - $y$  plane surrounding a given molecule are of a trivial nature, i.e., they mainly contribute to the Clausius-Mossotti local field correction to the dielectric function in a way well known for molecular crystals.<sup>24</sup> The image-force effect is greatest near the metal surface, and gradually decreases towards the bulk. Thus transport is determined by the mismatch in the LUMO energy near the layers charged by incoming carriers, and in the bulklike layers further upstream. The difference in the gap reduction near the metal-like and bulklike layers is found to be  $\sim 0.4$ - $0.5$  eV from the  $E_g$  values already given. This 0.4 eV is shared between the LUMO and the HOMO. The sharing may be equal, or 5:3 if weighted by the HOMO and LUMO degeneracies. (Thermal broadening and phonon effects are also relevant but would be smaller. The phonon associated with the deformation of a  $C_{60}$  from a sphere to a prolate ellipsoid involves only 33 meV. These processes contribute mostly to the imaginary part of the self-energy of the eigenvalues. That is, they contribute to the scattering processes which lead to the electrical resistance of the sample). Thus the LUMO mismatch forms a transport gap of  $\sim 0.15$ - $0.2$  eV. Also the molecular film is noncrystalline, and leads to some average value for the measured  $E_g$ .

In the usual picture of electron transport in molecular devices like:  $A/\text{Molecular-layer}/B$ , an electron is injected from the source electrode  $A$  into the LUMO of the nearest molecule, converting it to a transient, excited  $(M^-)^*$  anion. This involves Coulomb blockade, rearrangement of bond lengths, angles, etc., to give the actual  $M^-$  anion. At this point the carrier may become localized on the molecular site as a polaron—that is, the usual phononlike oscillations of the nuclei about their equilibrium positions become extremely anharmonic and the final equilibrium positions are established, stabilizing the charged ion. Space charges may develop. Then no conduction occurs until a suitably high bias is applied. Or, if the energy offsets are favorable, the carriers may move to neighboring molecules and successively move towards the drain electrode. In the devices discussed here, the fulleride layers for Al, Mg, and Ag are already populated at

the LUMO with up to  $\sim 1.8$  electrons. Then the first layer of  $C_{60}$ , i.e., the metal-fulleride layer polarizes the second layer and enables the hopping of electrons under the applied bias, since the mismatch in the adjacent LUMO energies is small. Thus the usual  $C_{60}$  van der Waals film behaves as a quasimetal. At sufficiently low  $T$  even the small LUMO mismatch ( $\sim 0.16$  eV) poses a barrier for transport and space-charge limited conduction appears when  $T$  is lowered. Our accurate temperature-dependent measurements are at present limited to the range 240–320 K.

Our explicit geometry optimization (Table I) for the energy of the ground state, and the anion or cation state with a charge carrier, are equivalent to treating the electron-phonon interaction to all orders in a phonon-type calculation where the polaron is constructed by including more and more phonons to pick up strong anharmonicities until a self-consistent all order summation of the perturbation series is achieved. The importance of such effects is recognized, e.g., within the alkali-doped fullerenes. Thus  $K_4C_{60}$  is an insulator due to bond-distortion effects. Also,  $K_6C_{60}$  is a band insulator since the six electrons per molecule fill the threefold LUMO. In our system, the LUMO of the film is only occupied to  $\leq 1.8$  electrons<sup>29</sup> per  $C_{60}$  molecule. Explicit calculations show that the Mulliken charges and the bond distortions are evenly distributed over the  $C_{60}$  such that strongly coupled polaronic effects (and the need to invoke a variable-range hopping mechanism) are negligible in our system. This is also evident when we consider that  $C_{60}$  molecules are in some sense electron droplets with an  $r_s=1.7$ , i.e., strong-screening systems which ensure that the charged structure is

structurally quite close to the original structure, even though the gap is modified. The experiments of Park *et al.*,<sup>6</sup> also show that there is no Coulomb blockade of the in-out transfer of an electron from a single  $C_{60}$  molecule near metal electrodes.

#### IV. CONCLUSION

Our experimental results on  $C_{60}$  films show hitherto unexpected quasimetallic  $I$ - $V$  behavior at ambient temperatures, when contacted with low-work function metals which are protected from reactions with the metal surface using ultrathin layers of LiF, or ensuring that hot metal is avoided in the fabrication process. The quasi-Ohmic behavior at ambient temperatures is found to be an activated conduction process with an activation energy of about 0.16 eV when the temperature dependence of the conduction is investigated. These results are explained by proposing that the strongly polarizable metal surfaces and fullerene molecules interact via image forces reducing the HOMO-LUMO gap, with partial charge transfer to the LUMO levels. The activation energy is interpreted as a slight energy mismatch between LUMO levels of the layers closest to the injecting metal electrode, and the layers further up steam. Molecular electronic-structure calculations are presented in support of this interpretation.

#### ACKNOWLEDGMENT

We thank George Sawatzky (UBC) for his valuable comments.

\*Email address: chandre.dharma-wardana@nrc.ca

<sup>1</sup>R. W. Lof, M. A. van Veenendaal, B. Koopmans, H. T. Jonkman, and G. A. Sawatzky, *Phys. Rev. Lett.* **68**, 3924 (1992).

<sup>2</sup>O. Gunnerson, *Rev. Mod. Phys.* **69**, 575 (1997).

<sup>3</sup>Kwanggyeao Lee, Hyunjoon Song, Bongsoo Kim, Joon T. Park, Sangwoo Park, and Moon-Gun Choi, *J. Am. Chem. Soc.* **124**, 2873 (2002).

<sup>4</sup>See R. F. Service, *Science* **302**, 556 (2003).

<sup>5</sup>A. Turak, D. Grozea, X. D. Feng, and Z. H. Lu, *Appl. Phys. Lett.* **81**, 766 (2002).

<sup>6</sup>H. Park, J. Park, A. K. L. Lim, E. H. Anderson, A. P. Alivisatos, and P. L. McEuen, *Nature (London)* **407**, 57 (2000), and references therein.

<sup>7</sup>C. Zeng, H. Wang, B. Wang, J. Yang, and J. G. Hou, *Appl. Phys. Lett.* **77**, 3595 (2000).

<sup>8</sup>J. Taylor, Hong Guo, and Jian Wang, *Phys. Rev. B* **63**, 121104 (2001).

<sup>9</sup>D. W. Owens, C. M. Alda, D. M. Poirier, and J. H. Weaver, *Phys. Rev. B* **51**, 17 068 (1995).

<sup>10</sup>D. Purdie, H. Bernhoff, and B. Reihl, *Surf. Sci.* **364**, 279 (1996).

<sup>11</sup>X. Lu, M. Grobis, K. H. Khoo, S. G. Louie, and M. F. Crommie, *Phys. Rev. Lett.* **90**, 096802 (2003).

<sup>12</sup>M. K.-J. Johansson, A. J. Maxwell, S. M. Gray, P. A. Brühwiler, D. C. Mancini, L. S. O. Johansson, and N. Martensson, *Phys. Rev. B* **54**, 13472 (1996).

<sup>13</sup>A. J. Maxwell, P. A. Brühwiler, A. Nilsson, N. Martensson, and P. Rudolf, *Phys. Rev. B* **49**, 10717 (1994).

<sup>14</sup>G. K. Wertheim and D. N. E. Buchanan, *Phys. Rev. B* **50**, 11 070 (1994).

<sup>15</sup>C. Cepek, A. Goldoni, and S. Modesti, *Phys. Rev. B* **53**, 7466 (1996).

<sup>16</sup>E. A. Katz, D. Faiman, S. Shtutina, B. Mishori, and Y. Shapira, *Electronic Properties of Novel Materials: XII* (AIP, New York, 1998), p. 527.

<sup>17</sup>Z. H. Lu, R. S. Khangura, M. W. C. Dharma-wardana, M. Z. Zgierski, and D. Ritchie, *Appl. Phys. Lett.* **85**, 325 (2004).

<sup>18</sup>S. Altieri, L. H. Tjeng, F. C. Voogt, T. Hibma, and G. A. Sawatzky, *Phys. Rev. B* **59**, R2517 (1999); M. Kiguchi, R. Arita, G. Yoshikawa, Y. Tanida, M. Katayama, K. Saiki, A. Koma, and H. Aoki, *Phys. Rev. Lett.* **90**, 196803 (2003).

<sup>19</sup>C. J. Huang, D. Grozea, A. Turak, and Z. H. Lu, *Appl. Phys. Lett.* **86**, 033107 (2005).

<sup>20</sup>H. B. Michaelson, *J. Appl. Phys.* **48**, 4729 (1977).

<sup>21</sup>M. Grobis, A. Wachowiak, R. Yamachika, and M. F. Crommie, *Appl. Phys. Lett.* **86**, 204102 (2005).

<sup>22</sup>N. D. Lang and W. Kohn, *Phys. Rev. B* **7**, 3541 (1973).

<sup>23</sup>R. Hesper, L. H. Tjeng, and G. A. Sawatzky, *Europhys. Lett.* **40**, 177 (1997); J. vandenBrink, M. B. J. Meinders, J. Lorenzana, R. Eder, and G. A. Sawatzky, *Phys. Rev. Lett.* **75**, 4658 (1995).

<sup>24</sup>A. F. Hebard, R. C. Haddon, R. M. Fleming, and A. R. Kortan,

- Appl. Phys. Lett. **59**, 2109 (1991).
- <sup>25</sup>P. A. Bruhwiler, A. J. Maxwell, P. Rudolf, C. D. Gutleben, B. Wastberg, and N. Martensson, Phys. Rev. Lett. **71**, 3721 (1993); **73**, 2938 (1994); M. B. J. Meinders, L. H. Tjeng, and G. A. Sawatzky, *ibid.* **73**, 2937 (1994).
- <sup>26</sup>GAUSSIAN 98, Revision A.9, M. J. Frisch *et al.* (Gaussian Inc., Pittsburgh, PA, 1998).
- <sup>27</sup>For the acronyms, basis sets, etc., see A. D. Becke, J. Chem. Phys. **98**, 5648 (1993); C. Lee, W. Yang, and R. G. Parr, Phys. Rev. B **37**, 785 (1988).
- <sup>28</sup>A. N. Pasupathy, R. C. Bialczak, J. Martinek, J. E. Grose, L. A. K. Donev, P. L. McEuen, and D. C. Ralph, Science **306**, 86 (2004).
- <sup>29</sup>B. W. Hoogenboom, R. Hesper, L. H. Tjeng, and G. A. Sawatzky, Phys. Rev. B **57**, 11939 (1998).